Bull. Mater. Sci., Vol. 36, No. 7, December 2013, pp. 1225–1230. © Indian Academy of Sciences.

Electrical and dielectric properties of TiO_2 and Fe_2O_3 doped fly ash

DEBASIS ROY, PARVEEN SULTANA, SUBHAJIT GHOSH, SUKHEN DAS* and PAPIYA NANDY
Physics Department, Jadavpur University, Kolkata 700 032, India

MS received 23 July 2012; revised 8 November 2012

Abstract. **Electrical properties of ceramic materials has become an area of increasing interest in research because these materials possess a great potential for solid-state devices. Conducting polymer composites have attracted considerable interest in recent years because of their numerous applications in a variety of electric and electronic devices. It has been observed that these materials possess a very high relative dielectric constant and high electrical properties at room temperature. Such a high dielectric constant is one of the important parameters in capacitor fabrication and a high electrical conductivity can be used for ionic batteries and electrochemical sensors.**

Keywords. **Scanning electron microscopy (SEM); X-ray diffraction (XRD); FTIR; electrical properties; dielectric properties.**

1. Introduction

Coal-based thermal power plants are necessary for the increased generation of electricity. The end product of coal from power plants are fly ash. The accumulated fly ash is a matter of great concern to our environment (Cioffi *et al* 1994). Hence, the disposal of fly ash is a great concern for the human race and researchers around the world are trying for greater utilization of fly ash. Use of fly ash in the production of building bricks and pozzolanic cements are already in practice (Dana *et al* 2004a, b; Cividanes *et al* 2010). Important value added products like wear resistant ceramic liner, glass ceramics and synthetic mullite have been made from fly ash. Replacement of expensive quartz fillers in ceramic tile composition by fly ash have been tried by many workers for products like whiteware, stoneware, insulators, etc. Fly ash can provide the strength and plasticity to the porcelain/ceramic clay during the formation stage and contribute to mullite formation after firing (Dayal 1959; Das *et al* 1996; Haldar 2003; Goyal *et al* 2011).

The conducting polymers have emerged as a new class of materials, because of their unique electrical, optical and chemical properties (Kulkarni *et al* 2000; Hanjitsuwan *et al* 2011). By proper doping, the conductivity of these materials can be varied from semiconducting to metallic regime, which has offered a new concept of charge transport mechanism.

2. Materials and experimental procedures

Coal-fly ashsample (FA) collected from Indian thermal power plants contained both amorphous components (mainly SiO_2, Al_2O_3) and crystalline components (mainly quartz and mullite). Metal oxides of Fe, Ti, Ca, Mg, K, etc and some oxides of trace elements like Sr, Ba, Zr, etc were also present in this sample.

The sample was sieved through 250 holes/cm^2 mesh to get fine grained uniform powder with an average grain size of 0·5−4 μm and washed several times. Then the sample was homogenously mixed with 3, 5 and 7% (w/w) of TiO_2 or with Fe_2O_3 by dry milling for 4 h and subsequently wet milling in a high energy planetary ball mill (Fritch P6) at 1200 rpm for 40 min using zirconium balls. The mixed samples were then dried at 70 °C for 48 h in an electric oven. The samples were sintered at 1400 °C in an electric furnace with a heating rate of 5 °C/min and 120 min of soaking time. The sample was cooled at a rate of 15 °C/min in the same atmospheric condition within the furnace. After cooling, the samples were ground in an agate mortar to a fine powder form and finally stored at room temperature for different analyses (Kumar *et al* 2001; Mansou 2005; Sultana *et al* 2012). The samples prepared for characterization work, i.e. XRD, FTIR, FESEM and dielectric properties are in powder form.

3. Analysis and instrumentation

Phase identification of the samples sintered at 1000 °C were analysed by X-ray powder diffractometer (model-D8, Bruker AXS, Wisconsin, USA) using CuKα radiation of 1·5418 Å and operating at 40 kV with a scan speed of 1 s/step.

The characteristic stretching and bending modes of vibration of chemical bonds of a sample can be effectively evaluated by spectroscopic methods. 1% sample was mixed with spectroscopy grade KBr, pelletized to form disc and analysed by FTIR spectroscopy (FTIR-8400S, Shimadzu).

*Author for correspondence (sukhendasju@gmail.com)

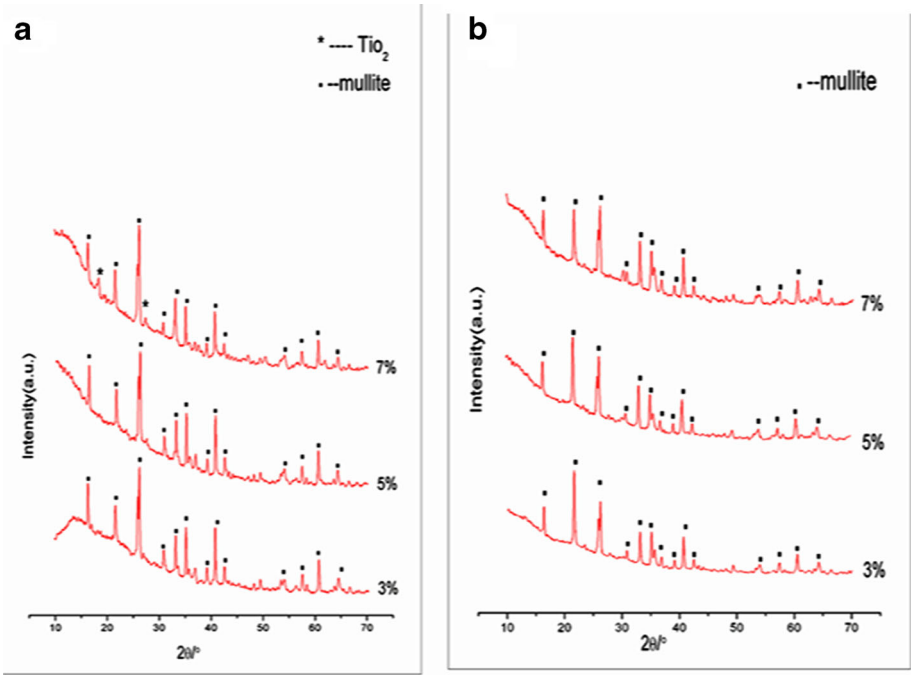

Figure 1. (a, b) X-ray diffraction pattern of FA-doped TiO_2 and Fe_2O_3 sintered at 1400 °C.

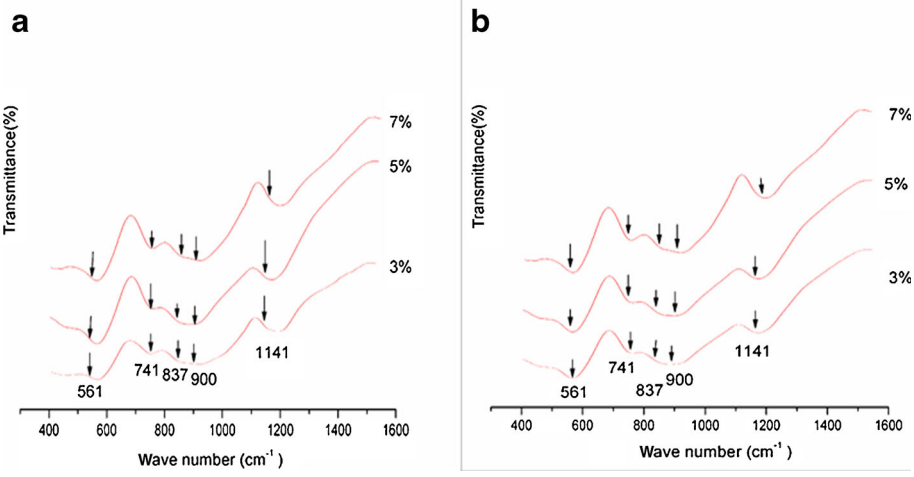

Figure 2. (a, b) FTIR bands of FA-doped TiO_2 and Fe_2O_3 sintered at 1400 °C.

The dielectric properties were determined by using LCR meter (HP Model 4274 A, Hewlett–Packard, USA) in the frequency range from 500 Hz–1·5 MHz, using the equation

$$\varepsilon_r = (C \times d)/A\varepsilon_o,$$

where C is the capacitance of the material, d is the thickness of the pellet and A is the area of cross-section. ϵ_r and ϵ_0 are the dielectric constant and permittivity of free space, respectively (Murugendrappa *et al* 2005; Mukhopadhyay *et al* 2010).

A.C. conductivity of the samples was estimated from the dielectric parameters. As long as pure charge transport mechanism is the major contributor to the loss mechanisms, a.c conductivity (σ_{ac}) may be calculated using the relation

$$\sigma_{a.c.} = 2\pi f \tan\delta\varepsilon_r\varepsilon_o,$$

where f is the frequency in Hz, tan δ is the dielectric loss factor, ϵ_r and ϵ_o are the dielectric constant of the material and permittivity of free space, respectively (Rohatgi *et al* 1997; Roy *et al* 2012).

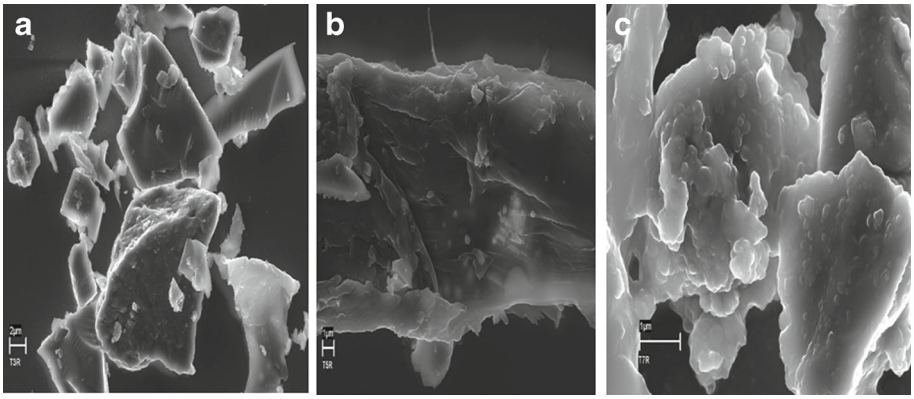

Figure 3. (a, b, c) FESEM of FA-doped TiO_2 doped at 1400 °C.

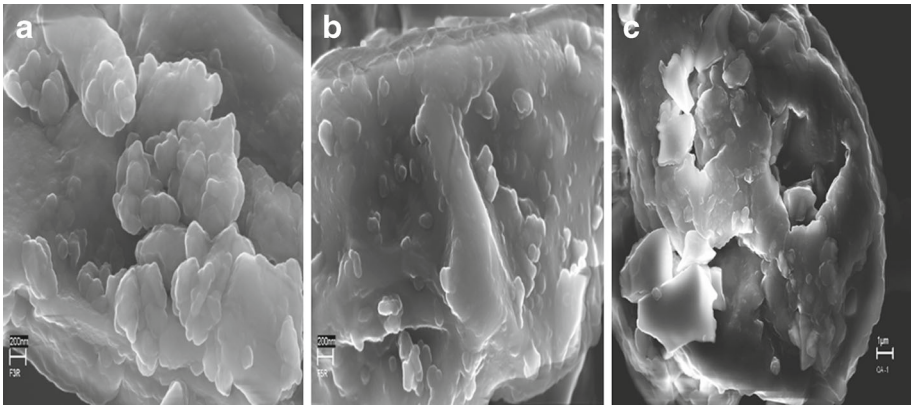

Figure 4. (a, b, c) FESEM of FA-doped Fe_2O_3 doped at 1400 °C.

Morphology of the sintered gels were observed by field emission scanning electron microscope (FESEM) (JSM 6700F, JEOL Ltd. Tokyo, Japan).

4. Results and discussion

4.1 *X ray diffraction analysis*

X-ray diffractograms of doped sintered gels show considerable enhancement in mullite phase at 1400 °C, respectively. The metal cations Ti^{2+} and Fe^{2+} have positive effect on the growth of mullite and increases with increase in concentration of the metal ion (figures 1a and b). The result indicates that the presence of metal cations reduces the activation energy of the reaction system and enhances the reaction rate of A_2O_3–SiO_2 to form mullite (Ravinder *et al* 2000).

The acceleration in mullite formation probably occurred because of sufficient decrease in viscosity of the glass phase due to the fluxing effect of metal ions. Interaction of the metal ion with alumina and silica component of the gel is implicated in accelerated transformation to mullite phase (Schneider *et al* 1994; Sindhu *et al* 2002).

From the diffractograms, it was found that with the increase in metal concentration of doped metal, phase transformation in the composite increases.

4.2 *FTIR analysis*

In FTIR analysis of the samples sintered at 1400 °C, figure 2(a and b) bands associated with mullite appear at around 560, 730, 820 and 1170 cm^{-1}. These bands correspond to 561(AlO_6), 741(AlO_4), 820(AlO_4), 1170(SiO_4), respectively. All the characteristic bands of mullite 561(AlO_6), 741(AlO_4), 837(AlO_4), 900(AlO_4) stretching mode and 1141 cm^{-1} (Si–O stretching mode) appear in samples (Oréfice and Vasconcelos 1997; Pandian and Krishna 2003).

4.3 *FESEM*

The morphology of 3, 5 and 7% (w/w) of TiO_2 and Fe_2O_3 treated fly ash is shown in figures 3(a–c) and 4(a–c).

Figure 3(a–c) indicates the micrograph of 1400 °C sintered TiO_2 fly ash sample and almost plate-like structure of mullite particle aggregation.

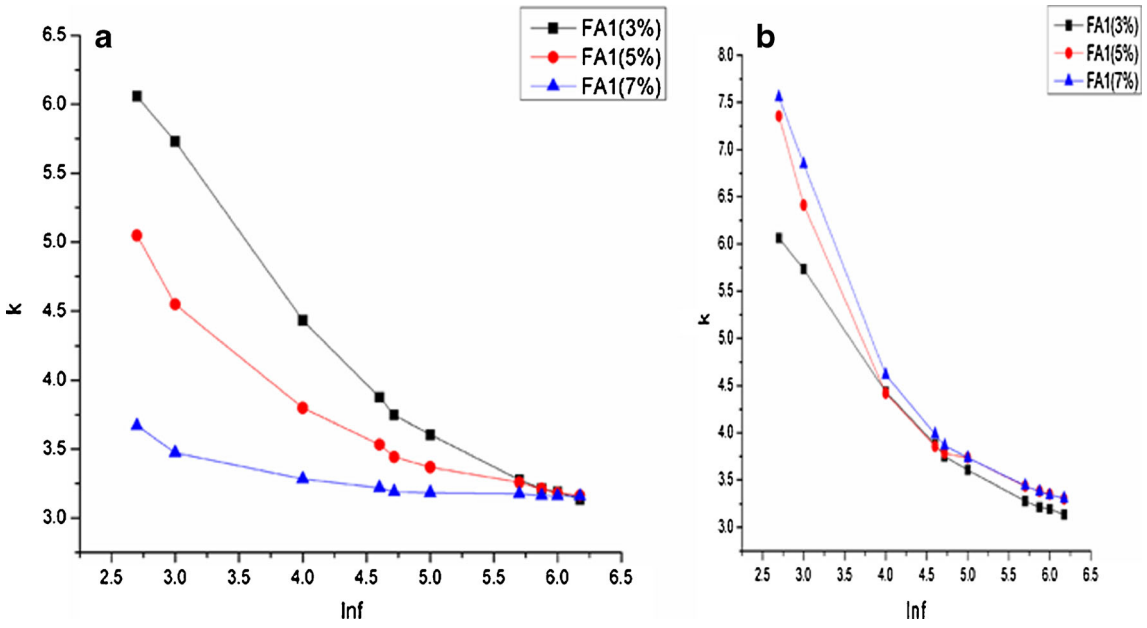

Figure 5. (a, b) Variation of dielectric constant with frequency (log f) of FA-doped TiO_2 and Fe_2O_3 sintered at 1400 °C.

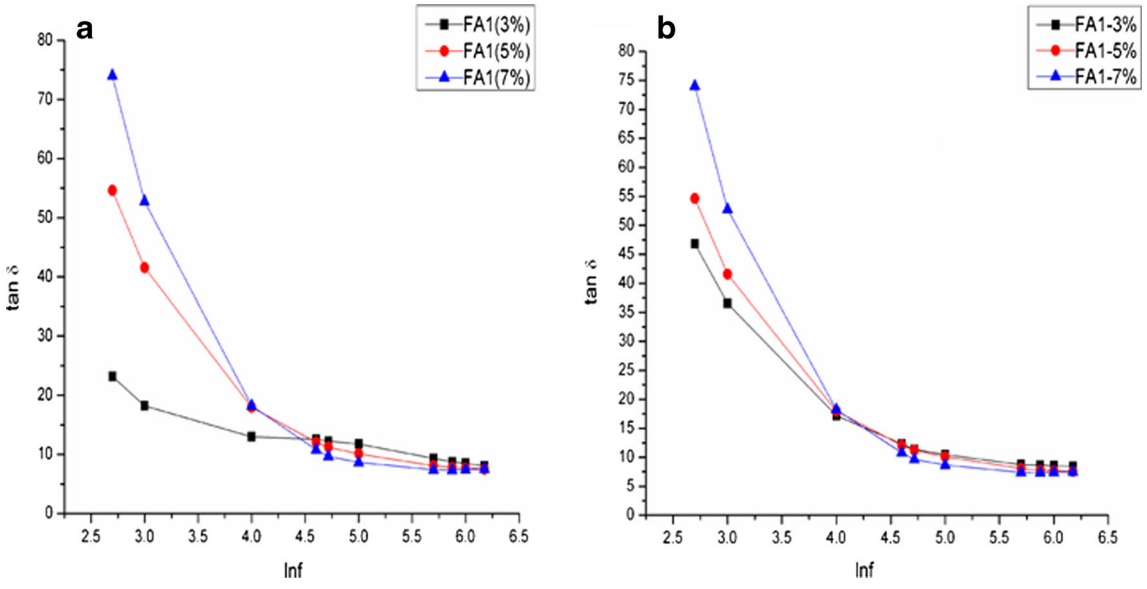

Figure 6. (a, b) Variation of dielectric loss tangent (tan δ) with frequency (log f) of FA-doped TiO_2 and Fe_2O_3 sintered at 1400 °C.

Figure 4(a–c) shows micrograph of Fe_2O_3 treated sample fired at 1400 °C.

The micrograph reveals the presence of numerous smaller particles along with amorphous aggregation.

4.4 *Dielectric measurements*

The variation of dielectric constant with frequency of FA-doped TiO_2 and Fe_2O_3 are shown in figure 5(a and b). From the plots, it has been observed that as the frequency increases, 'k' value decreases and attains saturation at 1·5 MHz for each concentration of doped TiO_2 and Fe_2O_3. This indicates a region of dispersion resulting from the relaxation of a polarization process within the system (Venkataraju *et al* 2010; Sultana *et al* 2011). The amorphous aggregation of mullite particles is due to the mineralizing action of doped TiO_2 and Fe_2O_3. It helps in controlling the internal individual dipoles in the presence of electric field and hence, controls the dielectric properties of the composite. The electronic polarizations

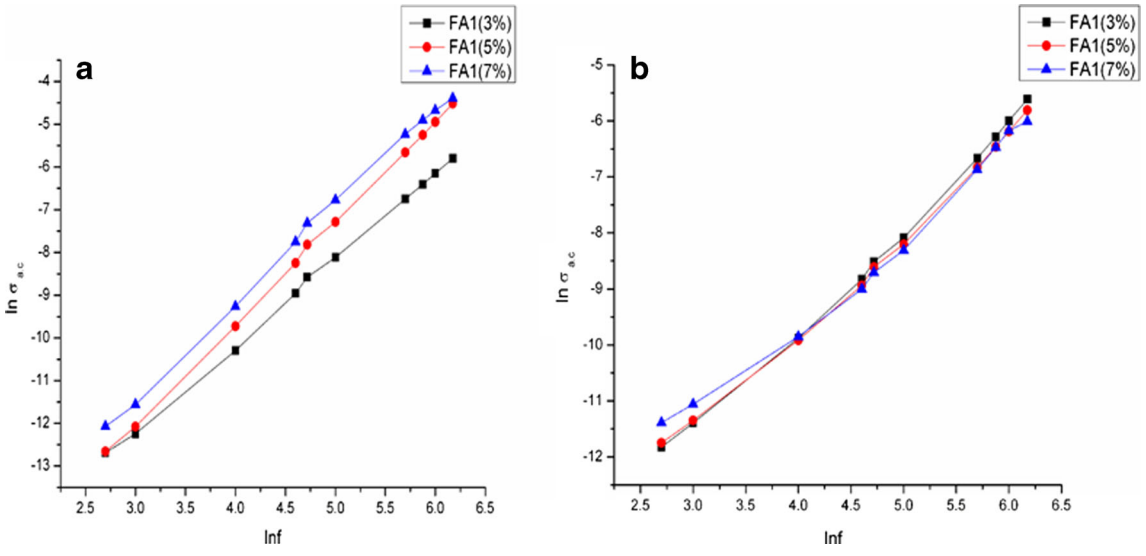

Figure 7. (a, b) Variation of a.c. conductivity ($\sigma_{a.c.}$) with frequency ($\ln f$) of FA-doped TiO_2 and Fe_2O_3 sintered at 1400 °C.

can orient themselves with the electric field at the lower frequency range, whereas higher frequency, the internal individual dipoles contributing to the dielectric constant cannot move instantly, so as frequency of an applied voltage increases, the dipole response is limited and the dielectric constant diminishes (Wang *et al* 2008; Venkataraju *et al* 2010).

The dielectric loss tan δ of each samples were measured in the frequency range 500 Hz–1·5 MHz at room temperature and is graphically shown in figure 6(a and b). At lower frequencies, tan δ is large for all samples except TiO_2 (3%) and decreases with increasing frequency. It reaches a constant value of 1·5 MHz. tan δ is the energy dissipation in the dielectric system. This behaviour of FA-doped TiO_2 and Fe_2O_3 is also due to the electrical polarization. At higher frequencies, the loss are reduced and the dipoles contribute to the polarization because the electronic polarizations can orient themselves with the electric field at lower frequency range and as frequency increases, the dipole response is limited and the dielectric loss tan δ also decreases.

Plot of ln $\sigma_{a.c.}$ vs ln f shows a linear increment of a.c. conductivity with frequency for all doping concentrations (figures 7a and b). This behaviour obeys the frequency dependent part of Jonscher's universal power law which can be represented by the equation

$$\sigma(\omega) = \sigma_{d.c.} + \sigma_0 \omega^S,$$

where $\sigma_{d.c.}$ is d.c. (or frequency independent) conductivity, σ_0 a temperature dependent parameter and s lies in the range $0 < s < 1$ and is applicable to the extended dispersion region (Yeledhalli *et al* 2007). Electrical conductivity as a function of frequency can be generally described as frequency independent, d.c. conductivity, $\sigma_{d.c.}$ and a strong frequency dependent components. With the increase in frequency, dielectric constant values decrease, whereas the conductivity values increase.

5. Conclusions

From the study, it can be concluded that the electrical conductivity and dielectric constant of FA doped TiO_2 and Fe_2O_3 are dependent on the frequency and doping percentage. The conductivity increases, but the dielectric constant decreases with the increase in frequency. The dielectric constant of the composites followed typical trend observed in ceramic materials, i.e. decreased with frequency for all the samples attaining constancy at high frequency (1·5 MHz). Similar nature was observed in case of dielectric loss (tan δ). A.C. conductivity of the composites increased with frequency following Jonscher's power law and was found to depend on the amount of amorphous phase and the hopping mechanism of mobile ions present in the composites. FA-doped TiO_2 and Fe_2O_3 having high dielectric constants also show high tangent loss. Variation in tan δ of FA-doped TiO_2 and Fe_2O_3 with different doping percentages is expected to be suitable for being developed as a fast ionic conductor.

Acknowledgments

We are grateful to the Department of Science and Technology and University Grant Commission (PURSE program), Government of India, for the financial assistance.

References

Cioffi R, Pernice P, Aronne A, Catauzo M and Quattroni G 1994 *J. Eu. Cer. Soc.* **13** 143

Cividanes L S, Campos T M B, Rodrigues L A, Brunelli D D and Thim G P 2010 *J. Sol–Gel Sci. Technol.* **55** 111

Dana K, Das S and Das S K 2004a *Bull. Mater. Sci.* **27** 183

Dana K, Das S and Das S K 2004b *J. Euro. Ceram. Soc.* **24** 3169

Das S K, Kumar S and Rao P R 1996 *National seminar EWM* (Jamshedpur: National Metallurgical Laboratory) **86**

Dayal U 1959 *J. Inst. Eng.* **76** 174

Goyal R K, Jadhav P and Tiwari A N 2011 *J. Electron. Mater.* **40** 1377

Haldar M K 2003 *Ceram. Int.* **29** 573.

Hanjitsuwan S, Chindaprasirt P and Pimraksa K 2011 *Internat. J. Miner. Metall. Mater.* **18** 94

Kulkarni A R, Lunkenheimer P and Loidl A 2000 *Mater. Chem. Phys.* **63** 93

Kumar S, Singh K K and Rao P R 2001 *J. Mater. Sci.* **36** 5917

Mansou S F 2005 *Egypt J. Solids* **28** 263

Mukhopadhyay T K, Ghosh S, Ghosh J, Ghatak S and Maiti H S 2010 *Ceram. Int.* **36** 1055

Murugendrappa M V, Khasim S and Ambika Prasad M V N 2005 *Bull. Mater. Sci.* **28** 565

Oréfice R L and Vasconcelos W L 1997 *J. Sol–Gel Sci. Technol.* **9** 239

Pandian N S and Krishna K C 2003 *J. Test. Eval.* **31** 479

Ravinder D, Prankishan G R M, Nitendarkishan P and Sagar D R 2000 *Mater. Lett.* **44** 256

Rohatgi P K, Guo R Q, Huang P and Ray S 1997 *Metal. Mater. Trans. A* **28** 245

Roy D, Bagchi B, Das S and Nandy P 2012 *J. Electroceram.* **28** 261

Schneider H, Okada K and Pask J 1994 *Mullite and mullite ceramics* (ed.) K Okada (Chichester: Wiley) p. 199

Sindhu S, Anantharaman M R, Thampi B P, Malini K A and Kurian P 2002 *Bull. Mater. Sci.* **25** 599

Sultana P, Das S, Bhattacharya A, Basu R and Nandy P 2012 *J. Appl. Ceram. Technol.* **9** 550.

Sultana P, Das S, Bhattacharya A, Basu R and Nandy P 2011 *Rev. Adv. Mater. Sci.* **27** 69

Venkataraju C, Sathiskumar G and Sivakumar K 2010 *J. Alloys Compd.* **498** 203

Wang S F, Wang Y R, Cheng K C, Chen J H and Hsaio Y P 2008 *J. Electron. Mater.* **37** 925

Yeledhalli N A, Prakash S S, Gurumurthy S B and Ravi M V 2007 *Karnataka J. Agric. Sci.* **20** 531